Tissue-mimicking phantoms for biomedical applications

Sieryi, Oleksii, Popov, Alexey, Kalchenko, Vyacheslav, Bykov, Alexander, Meglinski, Igor

Oleksii Sieryi, Alexey Popov, Vyacheslav Kalchenko, Alexander Bykov, Igor Meglinski, "Tissue-mimicking phantoms for biomedical applications," Proc. SPIE 11363, Tissue Optics and Photonics, 1136312 (12 May 2020); doi: 10.1117/12.2560174

SPIE.

Event: SPIE Photonics Europe, 2020, Online Only, France

Tissue-mimicking phantoms for biomedical applications

Oleksii Sieryi*, [1], Alexey Popov*,[2], Vyacheslav Kalchenko[3], Alexander Bykov*,[1], Igor Meglinski[1,4,5,6,7]

[1]Opto-Electronics and Measurement Techniques Unit, University of Oulu, Oulu, Finland; [2]VTT Technical Research Centre of Finland, Oulu, Finland; [3]Weizmann Institute of Science, Israel [4]Aston Institute of Materials Research, School of Engineering and Applied Science, Aston University, Birmingham, UK; [5]School of Life and Health Sciences, Aston University, Birmingham, UK; [6]Interdisciplinary Laboratory of Biophotonics, National Research Tomsk State University, Tomsk, Russia;[7]Institute of Engineering Physics for Biomedicine (PhysBio), National Research Nuclear University "MEPhI", Moscow, Russia

ABSTRACT

Emerging biomedical instrumentation for imaging and diagnostics requires tissue-mimicking phantoms with optical properties close to those of real biological tissues. Many such tissues and organs consist of several layers with different physical properties, e.g. the head includes the brain, skull, and skin, which in turn also comprise several layers. Structure, optical and mechanical properties depend on the purpose of phantoms and studied materials and technologies. In this paper, we present both plain single-, multi-layered phantoms, and complex opto-mechanical phantoms that imitate parts of the body, in particular, the head. We describe the procedure, materials, internal structure, and tuning of the optical properties of two different phantom manufacturing methods as well as show examples of tissue-mimicking phantoms for different biomedical applications.

Keywords: phantoms, tissue-mimicking, optical properties, head phantom, biomedical

1. INTRODUCTION

Tissue-mimicking phantoms play an important role in the development of biomedical instruments. Designing stable long-lasting and realistic phantoms of biological tissues is an important issue in biophotonics[1]. Increasing interest in optical techniques for noninvasive biomedical diagnostics and therapy leads to the development of new methods and devices[2]. A significant phase of such development is a validation of created systems, proposed methods, and theoretical predictions. A particularly important aspect of this field is imaging and sensing of cells and tissues as well as detecting blood circulation in vessels and capillaries. To achieve these goals manufacturing of single and multilayer phantoms with a fully functional embedded capillary network is of high necessity. Additionally, modeling vascular pathologies such as stenosis or aneurysm is important. This paper describes the previous research conducted by the Biophotonics group of the University of Oulu as well as includes our recent achievements in phantoms fabrication.

2. MATERIALS AND METHODS

Phantoms are composed of a matrix material, a scattering constituent, and an absorbing constituent. This allows for independent and rigorous control of light absorption and scattering. There are two main groups of phantoms depending on the means to achieve their light-scattering properties: those which rely on nano- or microparticle-induced scattering and those which possess intrinsic scattering due to an internal structure and/or composition. Achieving the desired scattering coefficient in nano- or microparticle-based phantoms is performed via the controlled addition of nanoparticles of a specific type, size, shape, and concentration[3]. Special attention should be paid to avoid particle sedimentation. The particle-free phantoms, with intrinsic scattering, are perfectly homogeneous and usually easier to produce, although their optical properties can be more difficult to control.

*E-mail: olexii.siery@oulu.fi, alexey.popov@vtt.fi, alexander.bykov@oulu.fi

Tissue Optics and Photonics, edited by Valery V. Tuchin, Walter C. P. M. Blondel, Zeev Zalevsky, Proc. of SPIE Vol. 11363, 1136312 · © 2020 SPIE
CCC code: 0277-786X/20/$21 · doi: 10.1117/12.2560174

2.1 Nanoparticles-based phantoms

As a host transparent medium, we used polyvinyl chloride-plastisol (PVCP)[4] (M-F Manufacturing Co., USA), which is a white opaque suspension of PVC particles in an oily substance that becomes transparent when heated at high temperatures. Scattering was introduced by adding submicron particles (Figure 1) either of zinc oxide[5] (ZnO) or titanium dioxide[6] (TiO_2) (Sigma-Aldrich, Germany) to PVCP before heating[7]. The superiority of ZnO over the widely used TiO_2 is caused by the value of the scattering anisotropy factor (g): for the size distribution of the used particles, the scattering anisotropy factor g was 0.8, while that of TiO_2 was 0.65 at the 900-nm wavelength. The amount of ZnO was calculated on the basis of the Mie scattering theory taking into account different particle sizes. PVCP with a certain amount of particles after sonication for 60 min was poured into a rectangular metal mold with flat walls and stored in an oven (heated to 180 °C) for 40 min[2]. Samples of phantoms of various shapes are shown in Figure 2.

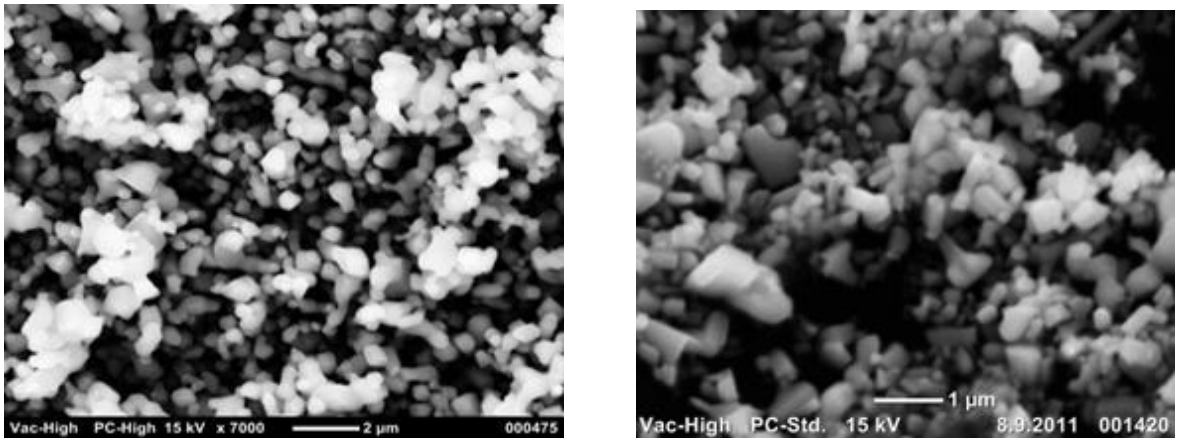

Figure 1. Scanning electron microscopy (SEM) images of the particles used to introduce scattering.

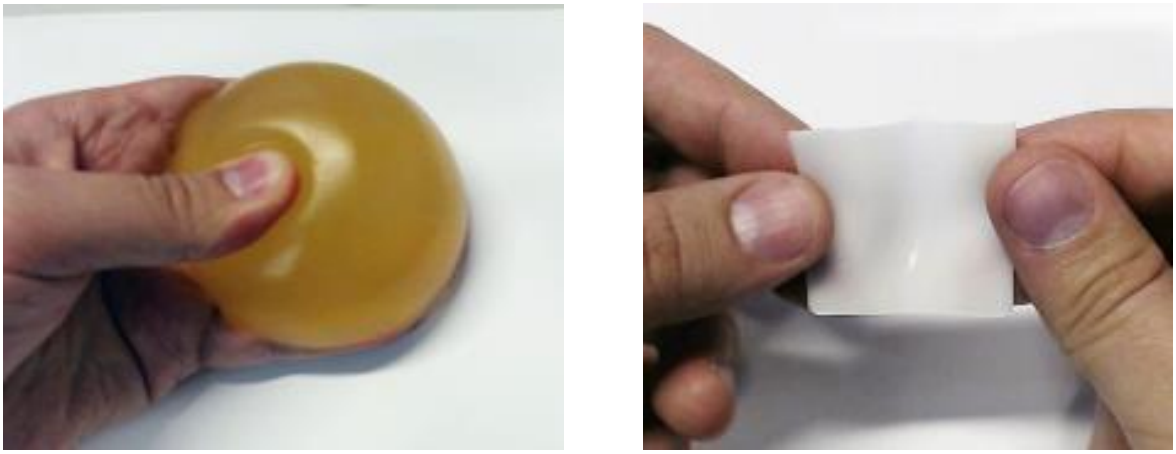

Figure 2. Plain and convex phantom layers with different absorption properties. Good flexibility and durability are demonstrated.

Further, the possibility of tuning the absorption properties of the phantom was investigated. Black absorbing pigment was added to PVCP at the volume concentration of 0.025% - 0.1% (Figure 3a). No scattering particles were administered at that time ($\mu_s \sim 0$). The absorption coefficient was estimated from the collimated transmittance measurements at a 900-nm wavelength using Beer's law. It was found that the absorption coefficient varies from 0.05 to 0.22 mm^{-1} for the selected range of the absorber concentrations (Figure 3b)[2].

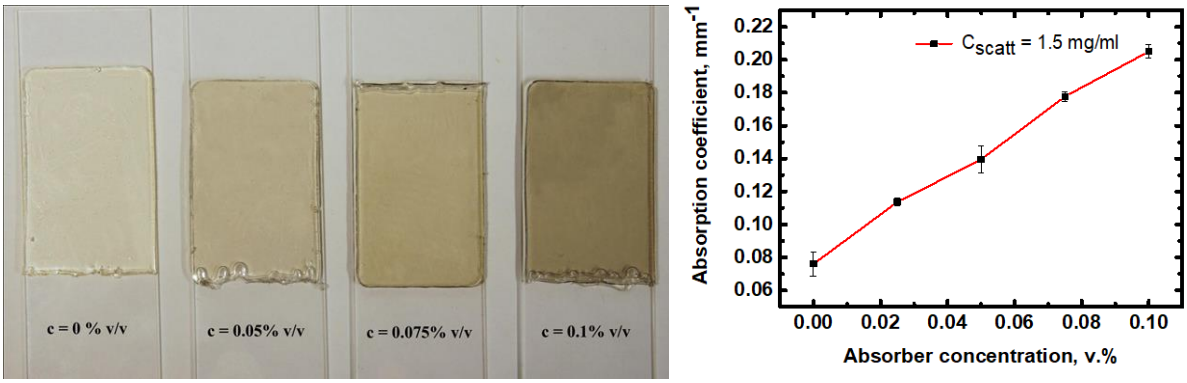

(a) **(b)**

Figure 3. Fabricated 1-mm-thick absorbing phantom layers with different concentrations of absorbing inks (a). Absorption coefficient of the same layers estimated from collimated transmittance measurements (b).

2.2 Silicone-based phantoms

An alternative to the conventional approach is represented by phantoms without scattering nanoparticles. In this case scattering is achieved by spherical cavities filled with glycerol naturally formed in the silicone matrix during manufacturing[3]. Below we describe optical properties and fabrication of such novel phantoms based on a mixture of silicone elastomer polydimethylsiloxane (PDMS) and glycerol (Figure 4)[8].

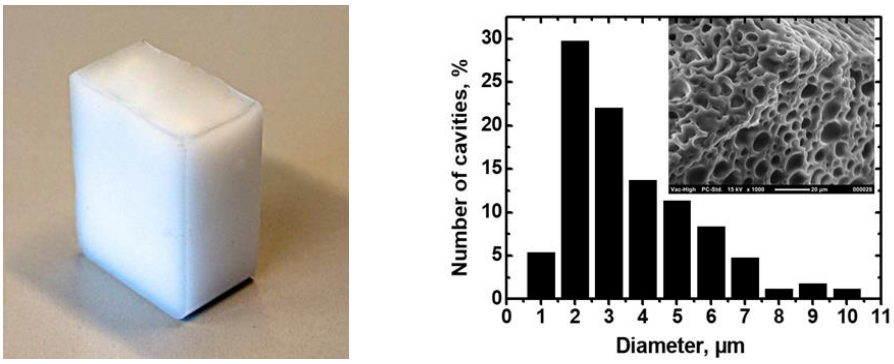

(a) **(b)**

Figure 4. A phantom slab (a). Size distribution of the intrinsic phantom cavities (b). The averaged cavity diameter in this case is ~4 µm. SEM image of the phantom structure (inset).

The phantom fabrication procedure is the following: first, the two components of PDMS are mixed together according to the manufacturers' proposed quantities of 10:1 parts by volume, a ratio of the base PDMS material to the curing agent volumes. Then, a required amount of glycerol is applied and carefully, thoroughly mixed, not to introduce excessive amounts of air. Air is evacuated from the mixture in a vacuum chamber. The mixture is poured into rectangular aluminum molds with controlled thickness. The standard process of the phantom fabrication requires no heating. The mixture is left at room temperature to solidify in less than 24 hours[3].

Optical properties and a structure of the manufactured phantoms depend on the content of the glycerol. Scanning electron images are depicted in Figure 5. The absorption coefficient stays rather constant. The scattering coefficient of the manufactured phantom varies from ~6 to ~10 mm^{-1}, which remains constant over the whole considered spectral range for at least 45 days.

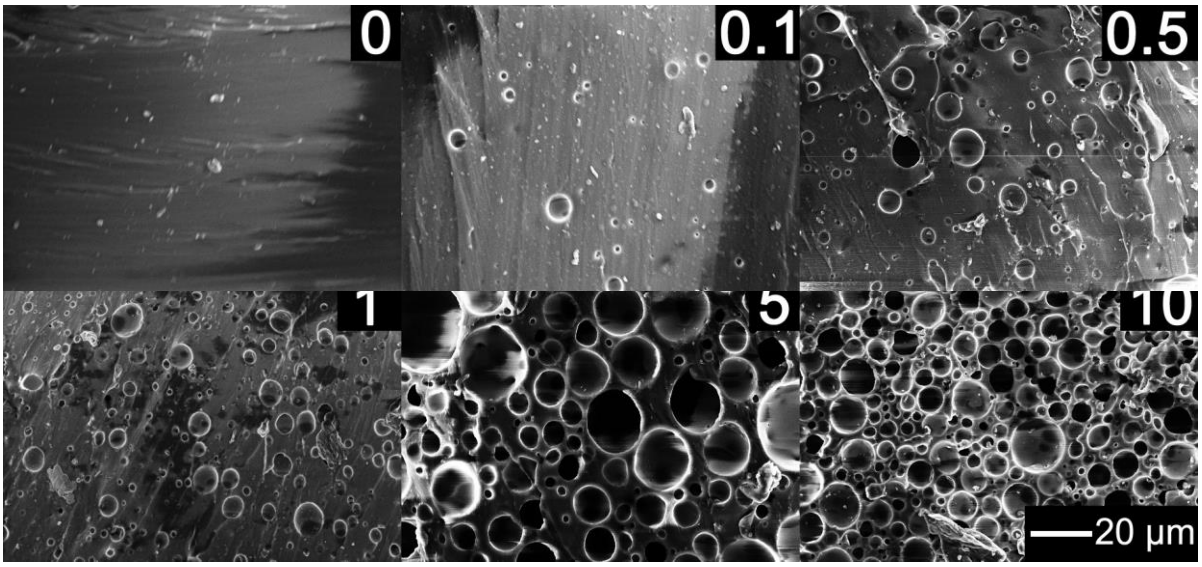

Figure 5. SEM images of the internal structure of phantoms with different glycerol content from 0 to 10 parts per volume, mixed with 10:1 parts per volume of PDMS to the curing agent.

3. RESULTS

Below are examples of produced tissue-mimicking phantoms for different biomedical applications. We present a fully functional capillary network embedded into a multilayered tissue phantom. PVCP was used as a host transparent medium. Scattering was introduced by adding TiO_2 submicron particles[2]. Another example is a head-mimicking opto-mechanical phantom consisting of skull and brain phantoms with appropriate optical and mechanical properties.

3.1 Multilayered tissue phantoms with an embedded capillary system

Using the nanoparticles-based approach we manufactured phantom layers of different thicknesses (0.3, 0.5, 1 and 5 mm). The multilayered 5-mm-thick phantoms were made as a composition of separate layers in different combinations. A capillary tree made of copper wires of different diameters (0.8, 0.4 and 0.2 mm) was inserted into the metal mold at a depth of ~1 mm before PVCP addition. Due to high elasticity of the solidified phantom material, it is possible to pull out the wires from the fabricated layer after its cooling without disrupting the capillary channels. The manufactured capillary channels in a transparent phantom layer are shown in Figure 6.

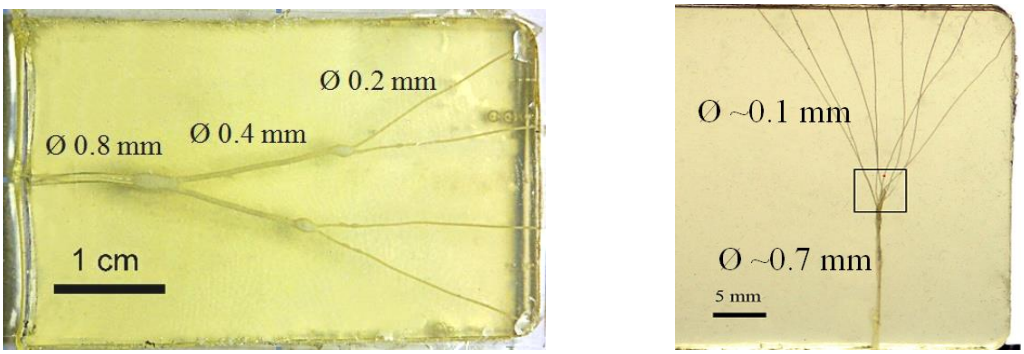

(a) **(b)**

Figure 6. Manufactured capillary system in a form of tree with several branches of different diameter in a phantom layer.

These channels can be filled with different liquids (e.g. Intralipid, blood, suspensions of particles) through a syringe needle and connected to a pump for Doppler optical coherence tomography (OCT) measurements (Figure 7). Using the method described above it is also possible to manufacture vessel structures mimicking pathologic states. In particular, by depositing an epoxy resin droplet of a certain diameter on the embedded wire an aneurysm-mimicking structure is realized. Removal of some material from the wire results in a converging vessel, which mimics the case of stenosis[2].

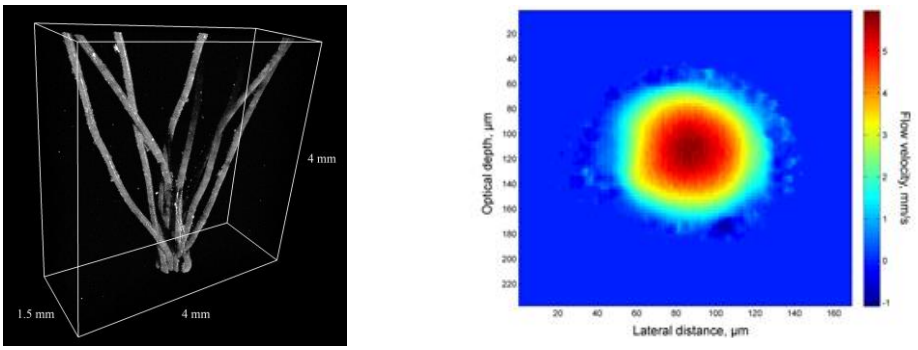

Figure 7. 3D OCT image of the capillary tree filled with Intralipid 4% (left) and map of the Intralipid flow velocity profiles measured with Doppler OCT technique inside one of the capillaries (right). The imaged area corresponds to the black rectangle shown in Figure 6b.

For preparing a scattering phantom we used TiO_2 particles (rutile, 650 nm average size). Proper amount of the particles was calculated according to the Mie theory assuming linear relationship between the scattering coefficient and the particle concentration. Three concentrations (1.5, 3 and 6 mg/ml) of TiO_2 particles correspond to the scattering coefficient of 2.5, 5 and 10 mm^{-1}, respectively. In order to control the absorption coefficient of the phantoms, CI Pigment Black 7 ink (M-F Manufacturing Co., USA) was added into PVCP before heat treatment. The concentration of the absorbing pigment varies within 0.025 - 0.1 % v/v.

3.2 Opto-mechanical phantoms

Utilizing recent achievements in material sciences, 3D printing technologies, and computer engineering, we aim to develop realistic tissue- and organ-mimicking phantoms with preset optical and mechanical properties to imitate the shape, size, softness etc. of the targeted tissue/organ. Depending on the selected materials and technological processes some parts of the phantom are 3D-printed, while the others can be molded, melted or milled. An example of a head-mimicking phantom is shown in Figure 8. The skull and brain are of real-size dimensions.

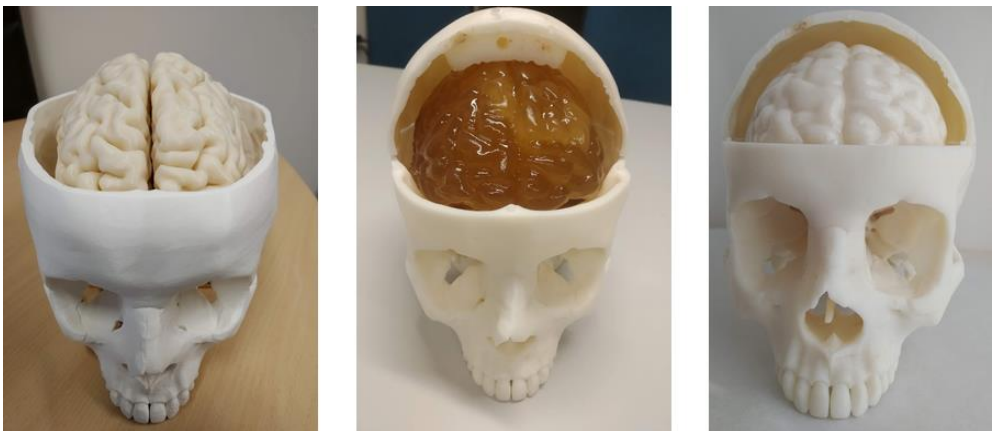

(a) **(b)** **(c)**

Figure 8. Head-mimicking phantoms comprising a 3D-printed skull with: (a) 3D printed solid-state brain, (b) flexible transparent brain, (c) flexible scattering brain.Optical properties for (c) correspond to the real situation at 800-nm wavelength[9].

The skull was printed using FDM technology with a plastic filament, which scattering and absorption are similar to the real optical properties of the human cranial bone tissue[9]. It is completely anatomically correct and of real size. Tuning of the skull phantom scattering property can be achieved by changing 3D printing settings such as resolution, orientation and density of the printing pattern etc. and depends on the 3D printer model and printing software. But the range that we can change in this case is not so large and is difficult to control. The key to success is the initial selection of plastic material with the targeted optical properties.

The other constituents of the head phantom (skin, gray matter, white matter) were fabricated using the nanoparticles-based technology described above and in our earlier publications[1,2,3], with PVCP as a matrix material and with zinc oxide (ZnO) nanoparticles as a scattering agent. The 'brain' was moulded from a two-sided silicone mold mimicking the shape of the human brain and the size corresponding to the skull phantom. Targeted optical properties and thickness of soft tissues were taken from literature[10-13].

For retrieval of optical properties of the fabricated phantom constituents the inverse adding-doubling[14] (IAD) method based on spectrophotometric measurements was utilized[15]. The results are presented in Figure 9. Satisfactory matching with the targeted properties was found.

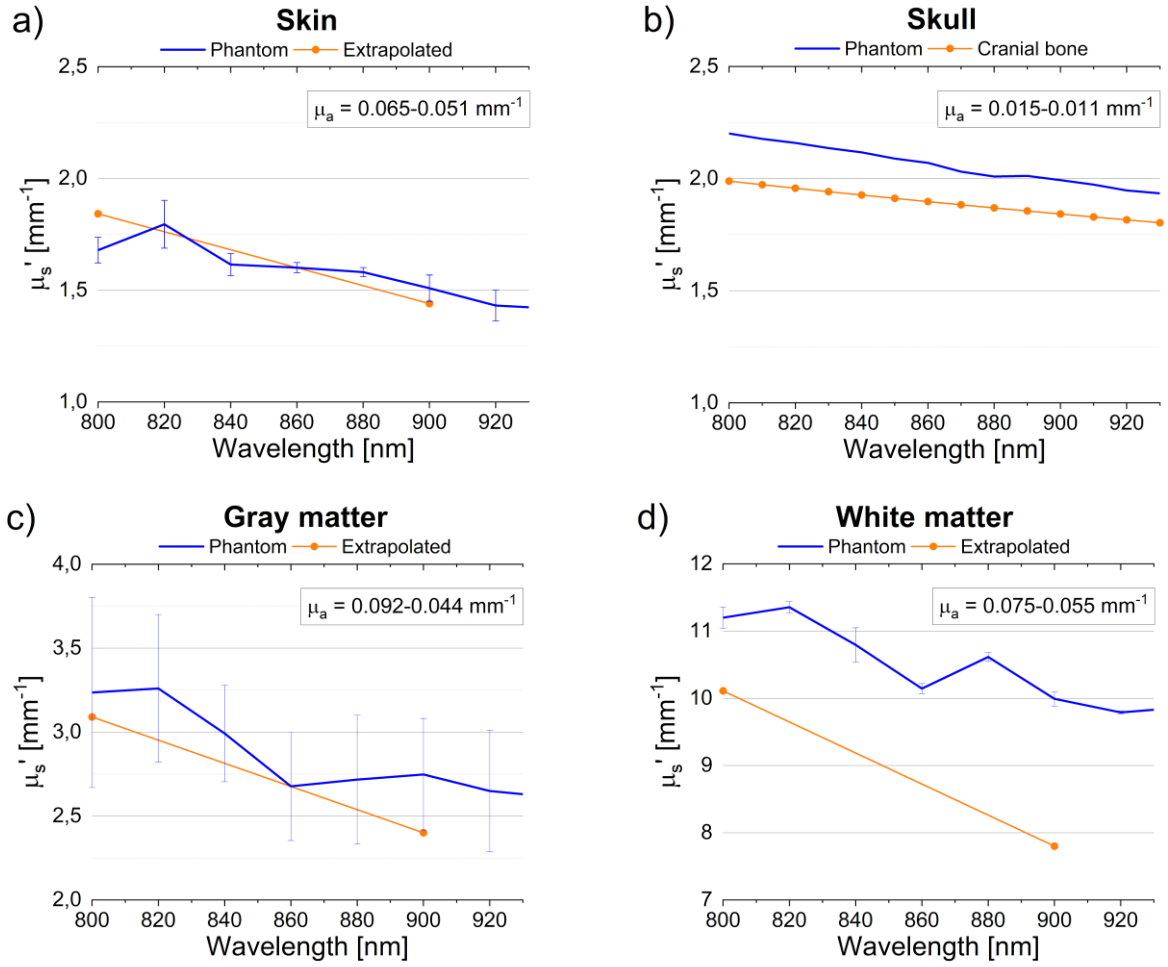

Figure 9. Reduced scattering coefficients of the head-mimicking layers (skin, skull, gray matte, white matter). Linear extrapolation is based on the single-scattering phantom measured at 900-nm wavelength ("Extrapolated"), and results of measurements of the fabricated phantoms simulating skin (a), skull (b), gray matter (c) and white matter (d).

This approach allows creating even more complex phantoms which are closer to real biological objects. Different tissue phantoms can be combined into one phantom mimicking a part of a body or a small animal. We also consider the possibility

of replacing parts of a phantom with inclusions with necessary optical properties, vascular or brain pathology, blood vessels parts etc. just like playing Lego. These kinds of phantoms are in high demand for developing brain sensors, design intracranial implants and other types of diagnostic medical devices.

4. CONCLUSIONS

The benefits of our phantom approach are the following:

- Large choice of optical and mechanical properties
- Customized surface roughness
- Tailored external and internal geometry (incl. distribution of tumors, hematomas, blood and lymph vessels etc.)
- Flexibility in the design and functionality
- Long-lasting stability

ACKNOWLEDGEMENTS

This project has received funding from the ATTRACT project funded by the EC under Grant Agreement 777222 and partially by Academy of Finland (grant: 325097, 314369). IM also acknowledges partial support from MEPhI Academic Excellence Project (Contract No. 02.a03.21.0005), Russian Science Foundation (Project 19-72-30012) and the National Research Tomsk State University Academic D.I. Mendeleev Fund Program.

REFERENCES

[1] A.V. Bykov, A.P. Popov, M. Kinnunen, T. Prykäri, A.V. Priezzhev, R. Myllylä, "Skin phantoms with realistic vessel structure for OCT measurements," Proc. SPIE 7376, 73760F (2010).
[2] A.V. Bykov, A.P. Popov, A.V. Priezzhev, R. Myllylä, "Multilayer tissue phantoms with embedded capillary system for OCT and DOCT imaging," Proc. SPIE 8091, 80911R (2011).
[3] M.S. Wrobel, A.P. Popov, A.V. Bykov, V.V. Tuchin, M. Jedrzejewska-Szczerska, "Nanoparticle-free tissue-mimicking phantoms with intrinsic scattering," Biomed. Opt. Express 7(6), 2088-2094 (2016).
[4] G.M. Spirou, A.A. Oraevsky, I.A. Vitkin, W.M. Whelan, "Optical and acoustic properties at 1064 nm of polyvinylchlorid-plastisol for use as a tissue phantom in biomedical optoacoustics," Phys. Med. Biol. 50, N141-N153 (2005).
[5] M.S. Wrobel, A.P. Popov, A.V. Bykov, M. Kinnunen, M. Jedrzejewska-Szczerska, V.V. Tuchin, "Multi- layered tissue head phantoms for noninvasive optical diagnostics," J. Innov. Opt. Health Sci. 8(03), 1541005 (2015).
[6] G. Lamouche, B.F. Kennedy, K.M. Kennedy, C.-E. Bisaillon, A. Curatolo, G. Campbell, V. Pazos, and D.D. Sampson, "Review of tissue simulating phantoms with controllable optical, mechanical and structural properties for use in optical coherence tomography," Biomed. Opt. Express 3(6), 1381-1398 (2012).
[7] B.W. Pogue and M.S. Patterson, "Review of tissue simulating phantoms for optical spectroscopy, imaging and dosimetry," J. Biomed. Opt. 11(4), 041102 (2006).
[8] D.M. de Bruin, R.H. Bremmer, V.M. Kodach, R. de Kinkelder, J. van Marle, T.G. van Leeuwen, D.J. Faber, "Optical phantoms of varying geometry based on thin building blocks with controlled optical properties," J. Biomed. Opt. 15(2), 025001 (2010).
[9] A.N. Bashkatov, E.A. Genina, V.I. Kochubey, V. V. Tuchin, "Optical properties of human cranial bone in the spectral range from 800 to 2000 nm," Proc. SPIE 6163 (2006).
[10] V. V. Tuchin, [Tissue Optics: Light Scattering Methods and Instruments for Medical Diagnosis], SPIE Press, Bellingham (2007).
[11] A. N. Bashkatov, E. A. Genina, V. I. Kochubey, V. V. Tuchin, "Optical properties of human skin, subcutaneous and mucous tissues in the wavelength range from 400 to 2000 nm," J. Phys. Appl. Phys. 38, 2543-2555 (2005).
[12] P. van der Zee, M. Essenpreis, D. T. Delpy, "Optical properties of brain tissue," Proc. SPIE 1888, 454-465 (1993).
[13] P. van der Zee, "Measurement and modelling of the optical properties of human tissue in the near infrared," PhD Thesis, University College London, London (1992).
[14] S.A. Prahl, M.J. van Gemert, A.J. Welch, "Determining the optical properties of turbid media by using the adding-doubling method," Appl. Opt. 32, 559-568 (1993).
[15] M.S. Wrobel, A.P. Popov, A.V. Bykov, M. Kinnunen, M. Jedrzejewska-Szczerska, V.V. Tuchin, "Measurements of fundamental properties of homogeneous tissue phantoms," J. Biomed. Opt. 20(4), 045004 (2015).